Design and simulation of a multi-input single output DC-DC converter using MATLAB Simulink.

Rekha BN[1], Dr. Ashok Kumar S[2], Lakshmi R[3], Priya[4], Nandini N[5]

*[1, 2, 3, 4, 5] Assistant Professor, Department of Electrical and Electronics Engineering, Bangalore Institute of Technology, Bengaluru-560004, India
Corresponding email ID: rekhabn85@gmail.com, ashokkumars@bit-bangalore.edu.in

Abstract:

This article proposes a high-gain, non-isolated, four-port DC-DC converter topology for hybrid energy applications. A multi-input single-output DC-DC converter is used to interface four power ports of three input ports and one output port. High output voltage gain, minimized component count, and high efficiency are the advantages of the proposed converter, which renders it very useful for hybrid energy applications, such as electric vehicle fast charging and DC microgrids. The high output voltage gain of the four port DC-DC converter is achieved using an actively switched inductor capacitor network. Moreover, a reduction in the component count is achieved by minimizing the number of switches per input port. The converter can provide the power demanded by the load in the absence of one or two sources.

Keywords: Capacitor network, power demand, hybrid energy, high efficiency, microgrid.

1. Introduction

Hybrid Electric Vehicles (HEV) and Electric Vehicles (EV) are becoming increasingly popular because of their environmental, socioeconomic, and health benefits (Verma et al., 2021). The reliance on renewable energy sources is growing as these vehicles become more accessible and simpler to implement. Photovoltaic (PV) energy is one of the most widely used renewable energy sources owing to its high efficiency and lack of spinning or moving parts. However, PV cannot provide electricity continually because it is dependent on solar irradiance. A battery and an ultra-capacitor are employed as extra sources to supply the converter with the required amount of power (Cheng et al., 2017). A multiport DC-DC converter architecture was designed for use in EV charging and DC microgrid applications (Ahmadi et al., 2015). Multiple-input converters (MICs) outperform traditional methods that use multiple single converters in terms of their performance. MICs are smaller and less expensive because they share active power switches, and reactive components increase power density (Xiao et al., 2021) MICs simplify power management with centralized control, reduce communication complexity, and improve dynamic performance. Because MICs are affordable and have promising development prospects, they are a great choice for EVs and grid-connected applications (Zhao & Heywood, 2017). To provide the required energy to the load, the provided converter, which is a multi-input converter, may integrate many sources, including solar PVs, batteries, and

ultracapacitors. Numerous studies have been conducted in this regard. However, a high duty cycle leads to increased conduction loss in the active switch and diode reverse recovery loss. In addition, the switch voltage stress is considerable and equal to the output voltage (Gutmann, 1999). Isolated converters, including forward, flyback, half-bridge, full-bridge, and push-pull types, can achieve substantial voltage gains by increasing the transformer turn ratio. However, difficulties, such as leakage inductance and parasitic capacitance, may arise in the secondary winding of the transformer (Baskar et al., 2020). This can generate voltage and current spikes, leading to increased voltage stress in the switching devices.

A multiport DC-DC converter topology is ideal for EV charging and DC microgrid applications. To provide the required energy to the load, the provided converter, being a multi-input converter, can integrate multiple sources, such an ultracapacitor, battery, solar photovoltaic system, etc. This non-isolated four-port DC-DC converter connects three input ports and one output port, making it ideal for electric vehicle charging and DC microgrid applications (see Fig.1). The Converter has five modes, allowing you to connect either supply to the load by changing the switching patterns.

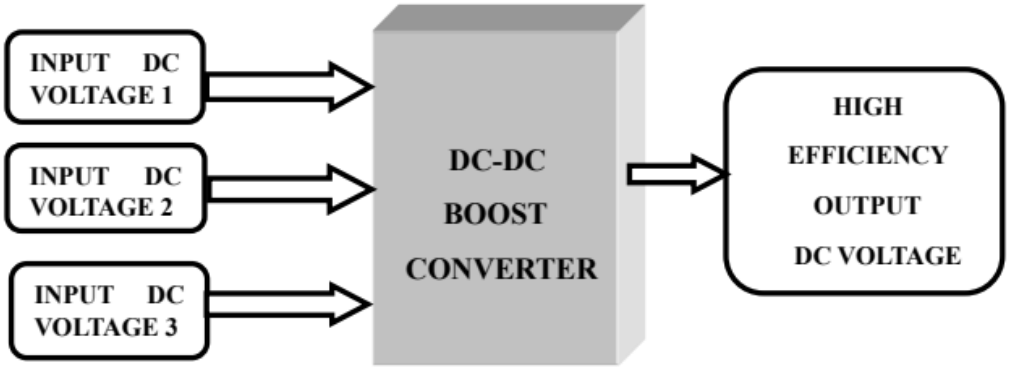

Fig 1: Block diagram of multiport DC-DC converter topology

2. Implementation and experimental procedure

DC-DC boost converters are commonly employed in a variety of applications, including renewable energy systems, electric cars, and portable devices. The implementation approach for a DC-DC boost converter typically consists of several main steps:

Design and choice of components: First, determine the appropriate input and output voltage ranges, power requirements, and switching frequency. Choose the right parts, such as the switching device (such as a GaN or MOSFET), diode, capacitor, and inductor. Achieving the intended voltage boost and reducing ripple depend heavily on the settings of the inductor and capacitor.

Control strategy: Select an appropriate control method, such as cascade control with inner current and outer voltage loops or more advanced techniques, such as Nonlinear Integral-Backstepping (NIB) combined with Model-Free Control (MFC), for dealing with constant power loads. Analog circuits or digital controllers will be used to implement the desired control strategy. Interestingly, various unique ways have been discovered to improve converter

performance. Furthermore, replacing the input inductance with an LCL filter reduces input current ripple, which is useful for sensitive power sources such as fuel cells and batteries. To sum up, putting a DC-DC boost converter into practice necessitates giving considerable thought to the design parameters, component choices, and control approach. Advanced techniques, such as voltage lift methods and switched-capacitor topologies, can be used to obtain higher voltage conversion.

2.1. The DC-DC Boost Converter

The boost converter is a DC-to-DC converter that performs step-up conversion of an applied DC input. The supplied fixed DC input is boosted (or enhanced) to an adjustable DC output voltage in the boost converter, resulting in an output voltage that is always greater than the input voltage. Therefore, another name for a boost converter is a step-up converter or step-up chopper. It is given the moniker "boost" because the generated output voltage is greater than the input voltage. It carries out the buck converter's opposite function, converting higher DC input into lower DC output. The boost converter is used to raise an input voltage to a greater level based on the load's needs. This step-up conversion in the boost converter is accomplished by storing energy in the inductor and releasing it to the load at a higher voltage. Boost converters are commonly employed in battery-powered systems where a pair of batteries deliver 3V but must power a 5V circuit. Since voltage and current are known to be multiplied to produce power, a rise in the boost converter's output voltage indicates a fall in the circuit's output current. At least one energy storage component, such as an inductor, capacitor, or both, and two semiconductors, such as a diode and transistor, are present. In boost converter circuits, additional semiconductor devices such as power MOSFETs, power BJTs, IGBTs, etc., are employed as switches.

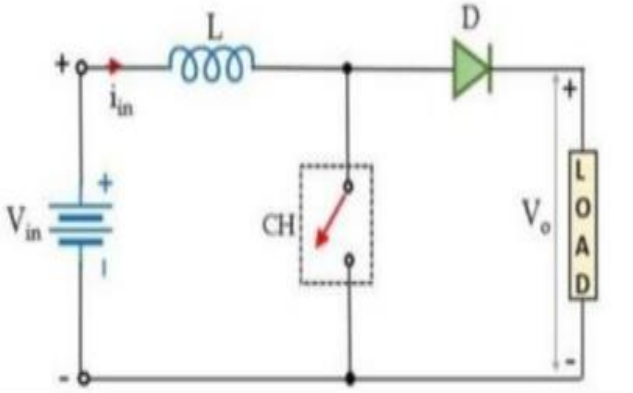

Fig 2: DC-DC Boost Converter

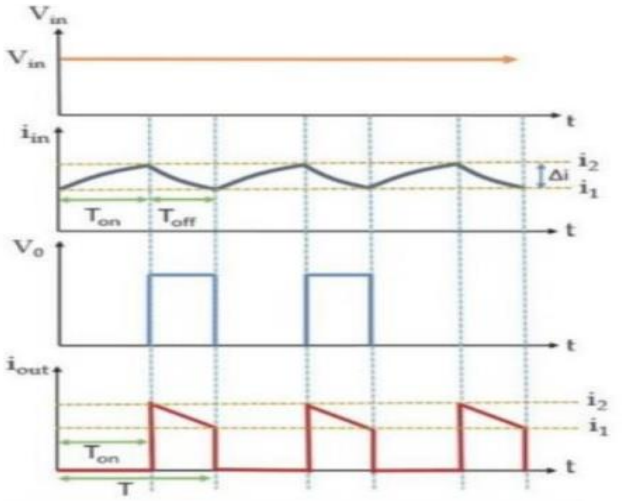

Fig 3: The waveform of the DC-DC boost converter

2.2. Multi-Input Single-Output DC-DC Converter

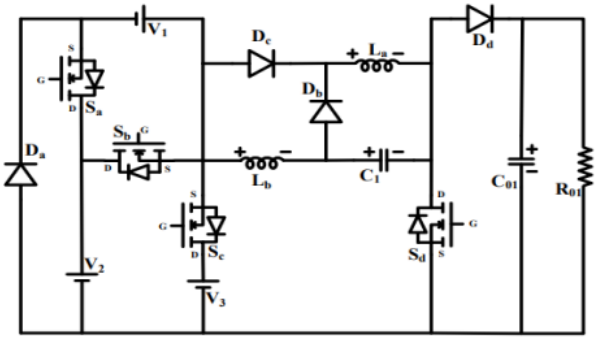

Fig 4: Circuit diagram for a multi-input single-output DC-DC converter

Fig. 4 shows the topology for the FPC. There are three input ports on this converter: V1, V2, and V3. The four power switches are designated as Sa, Sb, Sc, and Sd. It uses four power diodes, Da, Db, Dc, and Dd, to ensure the proper freewheeling path for the current during various modes of operation. Two inductors (La and Lb), two capacitors (C1 and C01), and a resistor (R01) serving as the load are the passive components used in the topology Together, inductor La, Lb, and capacitor C1 provide the intended high output voltage gain of the suggested converter. When it is isolated throughout various operating modes, capacitor C01 is used to supply the load.

Modes of Operation: This section discusses the different ways that this converter can operate. The following analogous circuits for each mode provide inductor voltage equations and capacitor current equations for the ideal situation.

Switches Sb and Sd are switched on in this mode, and the comparable circuit is depicted in Fig.6.Together with C1, 5 V2 charges the inductors La and Lb, and C01 feeds the load. At t = α1T, this mode starts, and at t = (α1 + α2)T, it finishes. The inductor voltage and capacitor formulae are shown below.

For Inductor voltage La: $V_{La} = V_1 + V_2$ (1)
For Inductor voltage Lb: $V_{Lb} = V_1 + V_2 + VC_1$ (2)
For Capacitor current IC_1: $IC_1 = I_{Lb}$ (3)
For Capacitor current $IC0_1$: $IC0_1 = -I0$ (4)

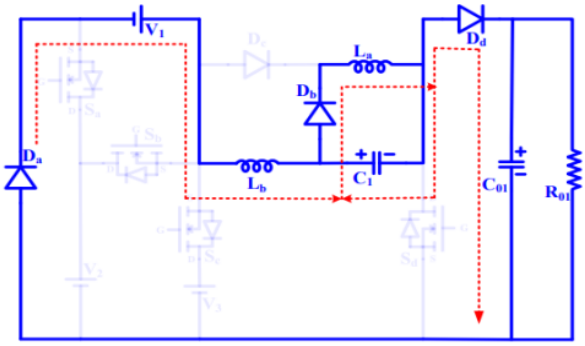

Fig 5: Circuit arrangement of Mode-1

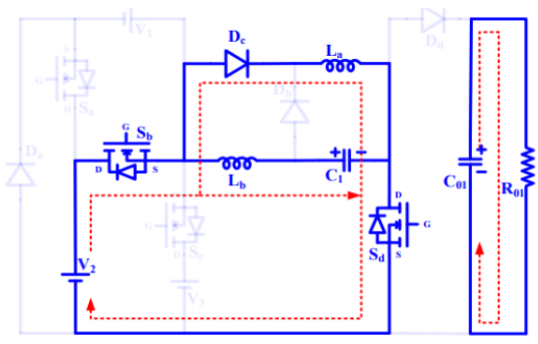

Fig 6: Circuit arrangement of Mode-2

Mode-I begins at t = 0, when switches Sa and Sd are turned ON, as depicted and its analogous circuit is shown in Fig. 5. In this mode, sources V1 and V2 are connected in series to charge inductors La and Lb. The load is supplied by capacitor C01. Until t = α1T, where T is the converter working time period as indicated by the frequency of operation, this mode remains in place. Capacitor C1 is charging with help from sources V1 and V2. The following formulas for the steady state inductor voltage and capacitor current are created. Switches Sb and Sd are switched on in this mode, and the comparable circuit is depicted in Fig.6.Together with C_1, 5 V_2 charges the inductors La and Lb, and C01 feeds the load. At t = α_1T, this mode starts, and at t = (α_1 + α_2) T, it finishes. The inductor voltage and capacitor formulae are shown below.

For Inductor voltage La: $V_{La} = V_2$ (5)
For Inductor voltage Lb: $V_{Lb} = V2 + VC_1$ (6)
For Capacitor current IC_1: $IC_1 = I_{Lb}$ (7)
For Capacitor current $IC0_1$: $IC0_1 = -I_0$ (8)

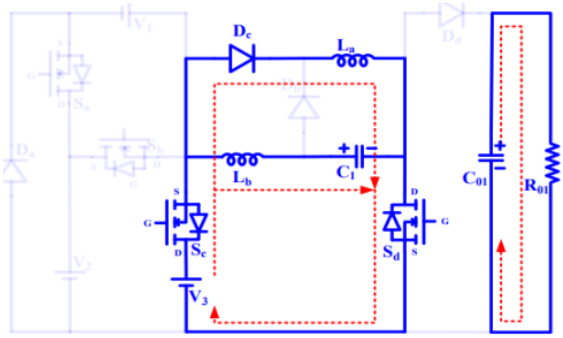

Fig 7: Circuit arrangement of Mode-3

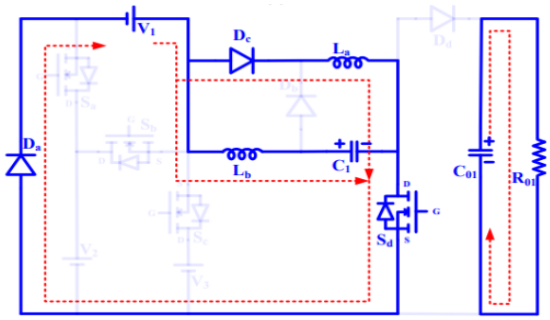

Fig 8: Circuit arrangement of Mode-4

Fig.7 depicts the analogous circuit for mode III. Switch Sc turns ON at t = (α_1 + α_2)T, whereas switch Sd remains ON from the preceding mode. In this instance, source V3 charges inductors La and Lb in addition to C1. C01 is the one who supplies the load. The anti-parallel diode in switch Sc will be forward biased in modes 1, 2, 4, and 5. However, in mode 3, the switch Sc is conducting, causing the antiparallel diode to be reverse biased. Thus, the anti-parallel diode across Sc will be reverse biased in this mode. This mode finishes at t = (α_1 + α_2 + α_3)T, and the inductor voltage and capacitor current formulae are listed below.

For Inductor voltage La: $V_{La} = V_3$ (9)
For Inductor voltage Lb: $V_{Lb} = V_3 + VC_1$ (10)
For Capacitor current IC_1: $IC_1 = I_{Lb}$ (11)
For Capacitor current IC01: $IC01 = -I0$ (12)
For Inductor voltage La: $V_{La} = V_1$ (13)
For Inductor voltage Lb: $V_{Lb} = V_1 + VC_1$ (14)
For Capacitor current IC_1: $IC_1 = I_{Lb}$ (15)
For Capacitor current $IC0_1$: $IC0_1 = -I0$ (16)

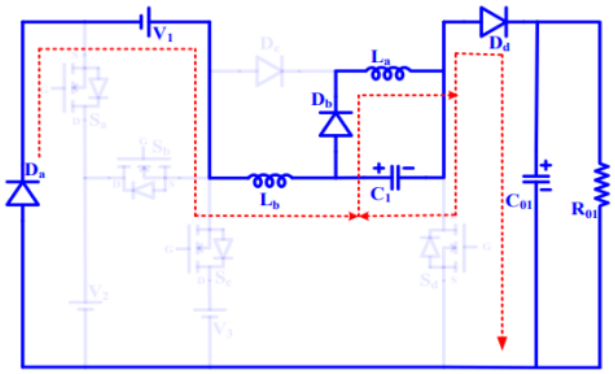

Fig 9: Circuit arrangement of Module-5

This is the last phase of converter operation, and the circuit structure is represented in Fig.9. In this state, all switches are switched off, and the load is linked via the diode Dd. Inductors La and Lb are connected in series with source V1 and provide power to the load. When discharging in this mode, the inductors' series-coupled configuration and constant charging are what cause the FPC's high output voltage. In addition, capacitor C1 is recharged by La. Starting at t = α4T, this mode continues until a full cycle is finished. The inductor La charges while the capacitor C1 is discharged, which contributes to the converter's gain. The inductor voltage and capacitor current formulae for this mode are shown below.

For Inductor voltage La: $V_{La} = -VC_1$ (17)
For Inductor voltage Lb: $V_{Lb} = V_1 + VC_1 - V0$ (18)
For Capacitor current IC_1 : $IC_1 = I_{Lb} = I_{La}$ (19)
For Capacitor current $IC0_1$: $IC0_1 = I_{Lb} - I0$ (20)

2.3. Four-Port Converter Analytical Waveforms

Fig.10 depicts analytical waveforms of inductor voltage, inductor current, and switch pulses of Sa, Sb, Sc, and Sd. At t=0, Sa is triggered for $\alpha_1 T$. After that, Sb is activated for a period of $\alpha_2 T$ at $t = \alpha_1 T$. Sc is operated for a time of $\alpha 3T$ following Sb.

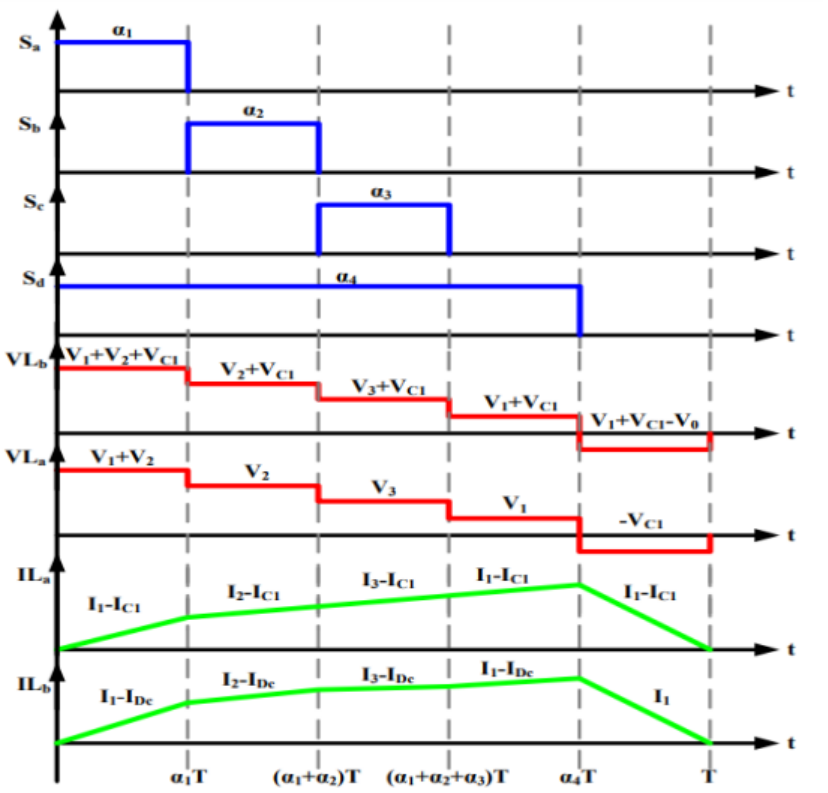

Fig 10: Waveform analysis of the four-port converter

At t = 0 with Sa, switch Sd is activated, and it stays ON for $\alpha_4 T$. All switches are off for the remainder of the time. Switches Sa, Sb, and Sc have duty ratios of 20% for α_1, α_2, and α_3, while switch Sd has a duty ratio of 70% for α_4. There are five voltage levels, four charging modes, and one discharging mode in the waveforms for both inductor voltages. The steady state inductor voltage calculations are used to create these waveforms. The inductors charge to various voltage levels for each mode before discharging in the fifth mode (Chen et al., 2011). Analytical inductor current waveforms are derived from the inductor voltage equation for each mode of operation, just as the inductor voltage waveforms. When both inductors are charged with the highest voltage in mode I, the current flowing through them increases. As the charging voltage drops, the inductor currents in modes II and III continue to rise, albeit with a smaller slope (Nomura et al., 2006). The current reaches its peak in mode IV, following which the current decreases and the inductors start to discharge.

2.4. Implementation of MATLAB SIMULINK

A high-performance language for technical computing, MATLAB combines computation, visualization, and programming. It is also a contemporary programming language environment with advanced data structures, integrated editing and debugging tools, and support for object-oriented programming, all of which make MATLAB a great teaching and research tool. Numerous computations are made possible by its robust built-in routines. Additionally, it features simple graphical instructions that enable instantaneous result visualization. Specific applications are grouped in bundles known as toolboxes. Toolboxes are available for a number of applied science and engineering domains, including simulation, control theory, signal processing, symbolic computation, and optimization.

3. Results and Discussion

The MATLAB/Simulink software simulates a multi-input, single-output DC-DC converter. To sum up, putting a DC-DC boost converter into practice necessitates giving considerable thought to the design parameters, component choices, and control approach (see Table 1). Advanced techniques, such as voltage lift methods and switched-capacitor topologies, can be used to obtain higher voltage conversion (see Fig.11).

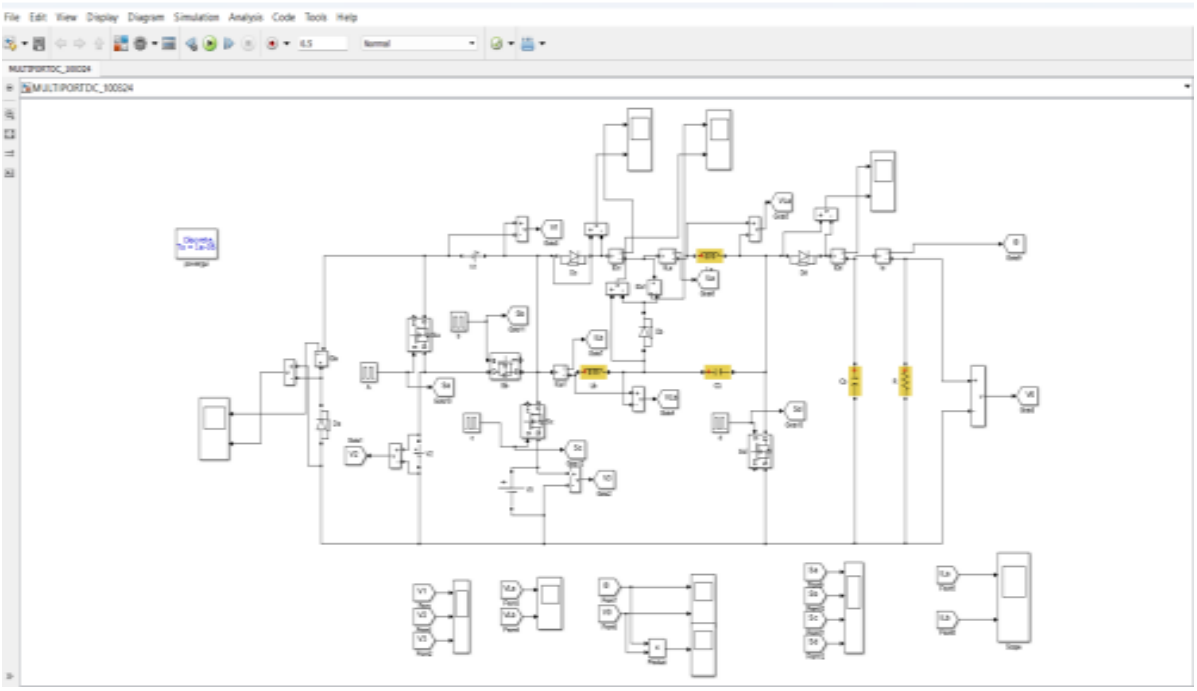

Fig 11: A simulation model for a DC-DC converter with several inputs and one output

Table 1: Simulation Input Parameters

Sl. No	Parameters	Specifications
1	Switching frequency	20KHz
2	Load Resistor (Ro)	300Ω
3	Capacitor (C1=C01)	100µF
4	Inductor (La=Lb)	5mH
5	Input Voltage(V3)	24V
6	Input Voltage(V2)	36V
7	Input Voltage(V1)	12V

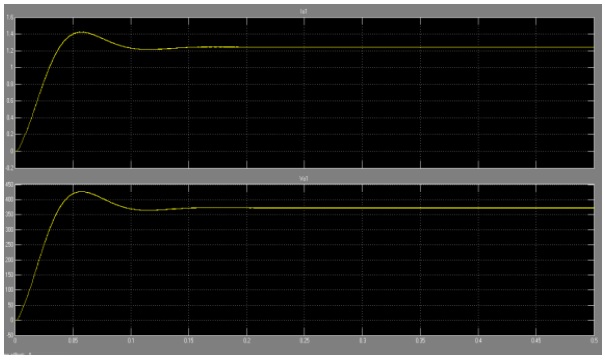

Fig 12: Output-Voltage and current simulation waveforms

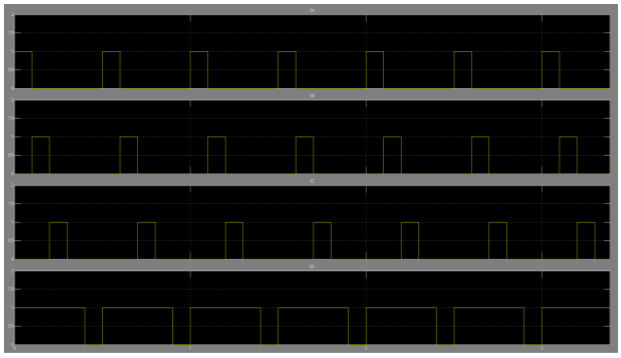

Fig 13: Effect of Switching pulses

Fig.12 to Fig.13 shows that switches pluses are Sa, Sb, Sc, and Sd have duty cycles of 20%, 20%, 20%, and 80%, respectively

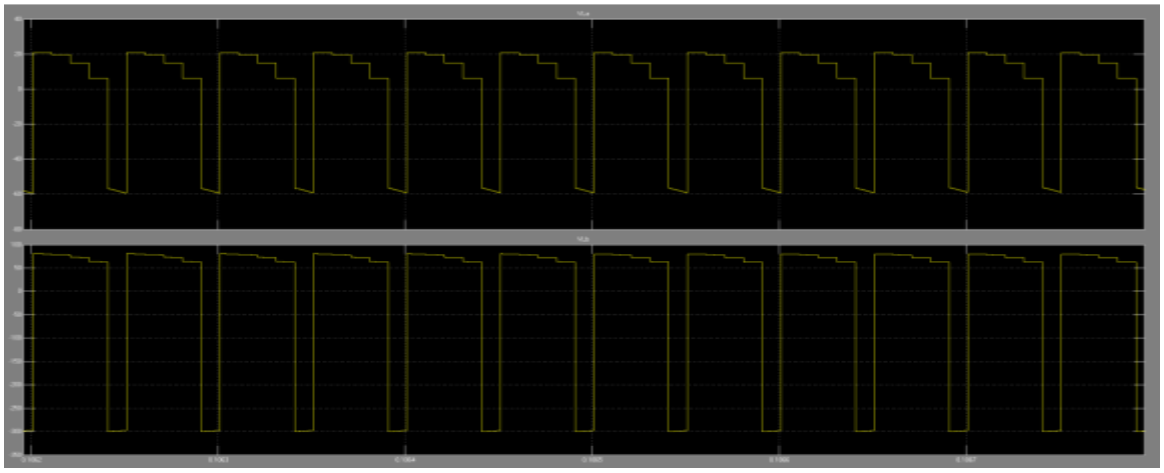

Fig14: Inductor voltage (VLa and VLb) simulation waveforms

Inductor La and Lb discharges at mode 5 after storing energy (charges) in modes I, II, II, and IV. The simulated inductor voltage and current waveforms presented here are identical to the analytical waveform (see Fig.14.to Fig.18).

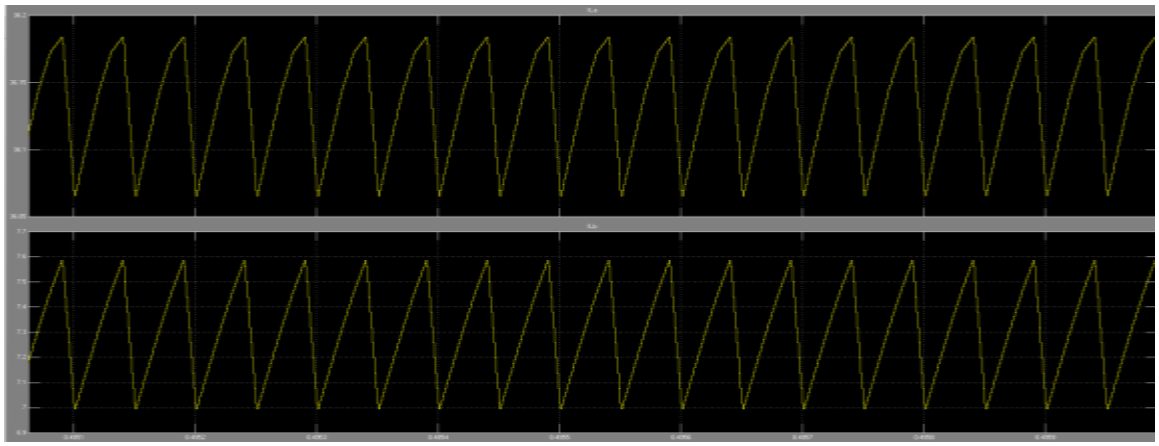

Fig 15: Simulation waveforms for inductor current (ILa and ILb)

The current through La has a peak value of 36.17A and a lowest value of 36.07A, whereas the current through Lb has a peak value of 7.58A and a lowest value of 7A.

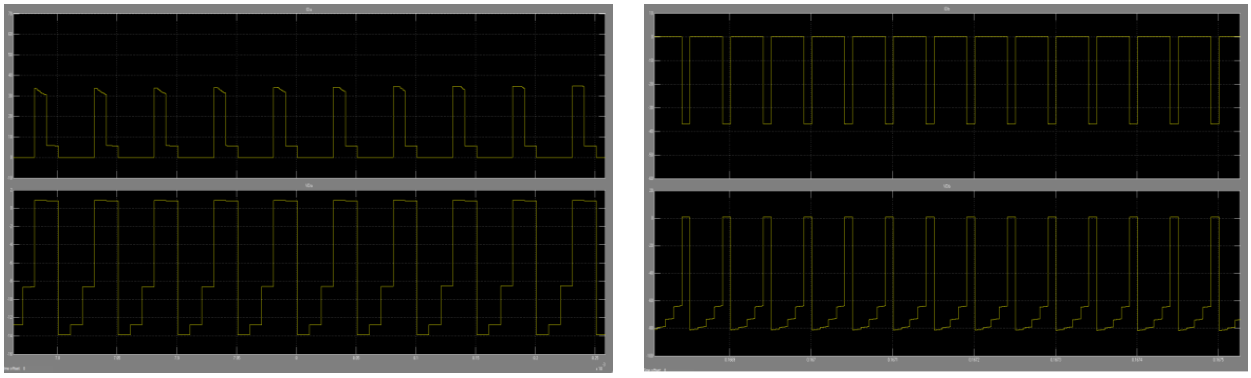

Fig 16: Waveforms of current and voltage simulations across Da and Db

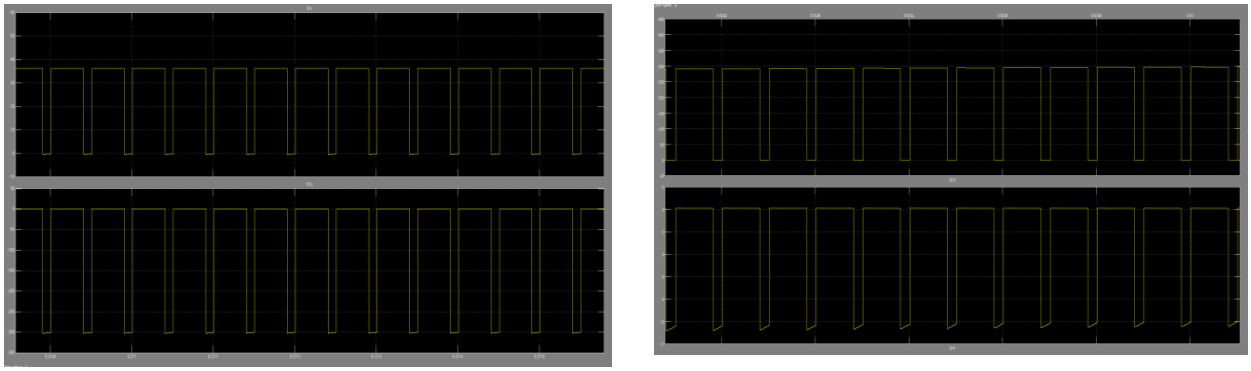

Fig 17: Simulation waveforms of Current and Voltage across Dc and Dd

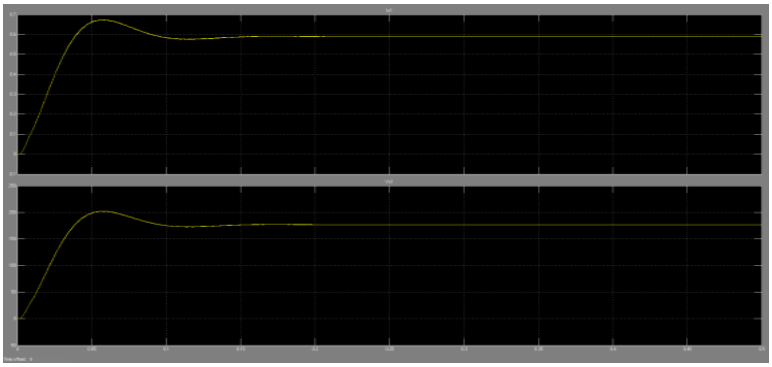

Fig 18: Current and voltage simulation waveforms for varying input values

4. Conclusion

The multi-input single-output DC-DC converter is simulated with three input sources with high voltage gain, low voltage stress across the switch, and common input and output grounding are among the converter's advantages. The voltages are 12V, 36V, and 24V input voltages result in an output of 370V. Without a transformer, the converter produces a voltage gain of 4.9 times. Only 20% (Sa, Sb, and Sc) and 80% (Sd) duty cycles are needed to accomplish the voltage gain. This converter has a high output voltage gain, great efficiency, and a small number of components. The converter structure can be adapted to act as a multiple input high-gain dc-dc converter, allowing it to interface with an unlimited number of input sources. Future study will focus on the converter structure for n-input and m-output, the impact of parasitic components on output voltage and efficiency, performance comparisons with recently reported similar topologies.

Acknowledgments

The authors are grateful to the Bangalore Institute of Technology for their valuable assistance in carrying out this work.

References

1. *Ahmadi, L., Croiset, E., Elkamel, A., Douglas, P. L., Entchev, E., Abdul-Wahab, S. A., & Yazdanpanah, P. (2015). Effect of socio-economic factors on EV/HEV/PHEV adoption rate in Ontario. Technological Forecasting and Social Change, 98, 93–104. https://doi.org/10.1016/j.techfore.2015.06.012*
2. *Baskar, S., V.Vijayan, V. V., Isaac Premkumar, I. J., Arunkumar, D., & Thamaran, D. (2020). Design and material characteristics of hybrid electric vehicle. Materials Today: Proceedings, 37, 351–353. https://doi.org/10.1016/j.matpr.2020.05.352*
3. *Bhaskar, M. S., Padmanaban, S., Ionel, D. M., Almakhles, D. J., Blaabjerg, F., & Subramaniam, U. (2020). Analysis and Investigation of Hybrid DC–DC Non-Isolated and Non-Inverting Nx Interleaved Multilevel Boost Converter (Nx-IMBC) for High Voltage Step-Up Applications: Hardware Implementation. IEEE Access, 8, 87309–87328. https://doi.org/10.1109/access.2020.2992447*
4. *Chellakhi, A., Abouelmahjoub, Y., & El Beid, S. (2021). Implementation of a Novel MPPT Tactic for PV System Applications on MATLAB/Simulink and Proteus-Based Arduino Board Environments. International Journal of Photoenergy, 2021, 1–19. https://doi.org/10.1155/2021/6657627*
5. *Chen, S.-M., Chen, J.-F., Yang, L.-S., & Liang, T.-J. (2011). A Cascaded High Step-Up DC–DC Converter with Single Switch for Microsource Applications. IEEE Transactions on Power Electronics, 26(4), 1146–1153. https://doi.org/10.1109/tpel.2010.2090362*
6. *Cheng, Y.-H., Teh, J., & Lai, C.-M. (2017, November 1). Memetic algorithm for fuel economy and low emissions parallel hybrid electric vehicles. https://doi.org/10.1109/icawst.2017.8256449*
7. *Dong, Z., Li, X. L., Li, Z., Tse, C. K., & Zhang, Z. (2021). Single-Inductor Multiple-Input Multiple-Output Converter With Common Ground, High Scalability, and No Cross-Regulation. IEEE Transactions on Power Electronics, 36(6), 6750–6760. https://doi.org/10.1109/tpel.2020.3036704*
8. *Gorji, S. A., Movahed, M., Ektesabi, M., & Sahebi, H. G. (2019, November 1). Multi-Input Boost DC-DC Converter with Continuous Input-Output Current for Renewable Energy Systems. https://doi.org/10.1109/ifeec47410.2019.9014953*
9. *Gunawardena, P., Nayanasiri, D., Hou, N., & Li, Y. (2023). A Dual-Input Single-Output DC-DC Converter Topology for Renewable Energy Applications. IEEE Transactions on Industry Applications, 59(2), 1995–2006. https://doi.org/10.1109/tia.2022.3218619*
10. *Gutmann, G. (1999). Hybrid electric vehicles and electrochemical storage systems — a technology push–pull couple. Journal of Power Sources, 84(2), 275–279. https://doi.org/10.1016/s0378-7753(99)00328-6*
11. *Irmak, E., & Guler, N. (2017). Application of a boost based multi-input single-output DC/DC converter. 4, 955–961. https://doi.org/10.1109/icrera.2017.8191200*
12. *Jaisiva, S., Premkumar, M., Jayakumar, V., Viji, K., Kumar, C., & Lakshmanan, M. (2022). Enhancement of Voltage Conversion Ratio using DC-DC Boost Converter with Coat Circuit. 60, 1–5. https://doi.org/10.1109/c2i456876.2022.10051308.*